(This is a sample cover image for this issue. The actual cover is not yet available at this time.)

Quaternary Science Reviews 43 (2012) 94–102

Contents lists available at SciVerse ScienceDirect

Quaternary Science Reviews

journal homepage: www.elsevier.com/locate/quascirev

Provenance of loess deposits in the Eastern Qinling Mountains (central China) and their implications for the paleoenvironment

Hongyan Zhang [a], Huayu Lu [a,*], Shao-Yong Jiang [b], Jef Vandenberghe [a,c], Shejiang Wang [d], Richard Cosgrove [e]

[a] School of Geographic and Oceanographic Sciences, Institute for Climate and Global Change Research, Nanjing University, Nanjing 210093, China
[b] State Key Laboratory for Mineral Deposits Research, School of Earth Sciences and Engineering, Nanjing University, Nanjing 210093, China
[c] Institute of Earth Sciences, VU University, 1081 HV, Amsterdam, The Netherlands
[d] Joint Laboratory of Human Evolution and Archaeometry, Institute of Vertebrate Paleontology and Paleoanthropology, Chinese Academy of Sciences, Beijing 100044, China
[e] Archaeology Program, School of Historical and European Studies, La Trobe University, Victoria 3086, Australia

A R T I C L E I N F O

Article history:
Received 15 August 2011
Received in revised form
28 March 2012
Accepted 11 April 2012
Available online

Keywords:
Eastern Qinling Mountains
Chinese Loess Plateau
Loess provenance
East Asian monsoon
Paleolithic

A B S T R A C T

Loess deposits in the Eastern Qinling Mountains (central China) provide a detailed archive for reconstructing the paleoenvironment during early hominin occupation. The study of the loess deposits also provides a unique opportunity to understand Pleistocene atmospheric circulation in this transitional climatic zone. However, the provenance and formation of the loess deposits were not well understood until now. In this paper, we report on new geomorphologic investigations and depositional analyses of the loess deposits. The results suggest that Gobi deserts and drylands in northern and northwestern China were one of the dust sources. These loess deposits show similar geochemical composition as the average upper crust (UCC), and may indicate that they experienced multiple sedimentary processes, with the dust being well mixed before deposition. However, the higher $^{87}Sr/^{86}Sr$ ratios (between 0.719650 and 0.721043) and extremely low $\varepsilon_{Nd}(0)$ values (between −11.98 and −18.97), which are different from the typical loess of the Chinese Loess Plateau, demonstrate that proximal clastic sediments that were apparently derived from the weathered Qinling orogen bedrocks, form the other important source for the loess deposits. The chemical Index of Alteration [$CIA = Al_2O_3/(Al_2O_3 + CaO^* + Na_2O + K_2O) \times 100$] and Chemical Proxy of Alteration [$CPA = 100 \times Al_2O_3/(Al_2O_3 + Na_2O)$], both in molar proportions show that the loess has experienced intense pedogenesis. We conclude that the loess deposit has a mixed provenance. The palaeoclimate in the Eastern Qinling Mountains remained mild in the glacial periods due to the topography and unique geographic locations, providing a suitable place for hominine occupation.

1. Introduction

Heavy dust storms occur in the arid-semiarid region of northern China every year, impacting heavily on the local and regional environment. The dust has even been detected in southeastern China, an area of subtropical monsoon climate (Li X.S. et al., 2009). The Gobi deserts have been traditionally considered as an important source of the dust, which was transported by northwesterly near-surface winds (the east Asian winter monsoon) and mainly deposited on the Chinese Loess Plateau (CLP) (Fig. 1A) (Liu, 1985; Liu and Ding, 1998; Guo et al., 2000; Nugteren and Vandenberghe, 2004; Yang et al., 2007a, 2008; Vriend et al., 2011). However, many researchers also have suggested that the Gobi desert was not the only source of the loess. The piedmont alluvial fans and drylands in north China also play a vital role in dust emission (Guan et al., 2008; Stevens et al., 2010; Weissmann et al., 2010; Yang et al., 2011) and until recently, the source, transport mechanism and deposition of the loess deposits in places other than the CLP was investigated (Hao et al., 2010; Yang et al., 2010; Qiao et al., 2011).

The Qinling Mountain Belt (QMB) is located in central China, south of the CLP (Fig. 1A). Presently, the two sides of the QMB have distinctly different climates and vegetation cover. The south side has a subtropical climate with a fertile landscape supporting dense vegetation while the north side is semiarid with sparse vegetation cover. The QMB is traditionally considered to have blocked dust transport from the northwest to southeast China that led to the belief that less loess was deposited in the south of the QMB. However, well-preserved loess has been found in the Eastern Qinling Mountains (EQLM) (Lei, 1998, 2000; Lu et al., 2007) and investigations into the origin and formation of these deposits have

* Corresponding author. Tel.: +86 25 83686740.
E-mail address: huayulu@nju.edu.cn (H. Lu).

0277-3791/$ – see front matter © 2012 Elsevier Ltd. All rights reserved.
doi:10.1016/j.quascirev.2012.04.010

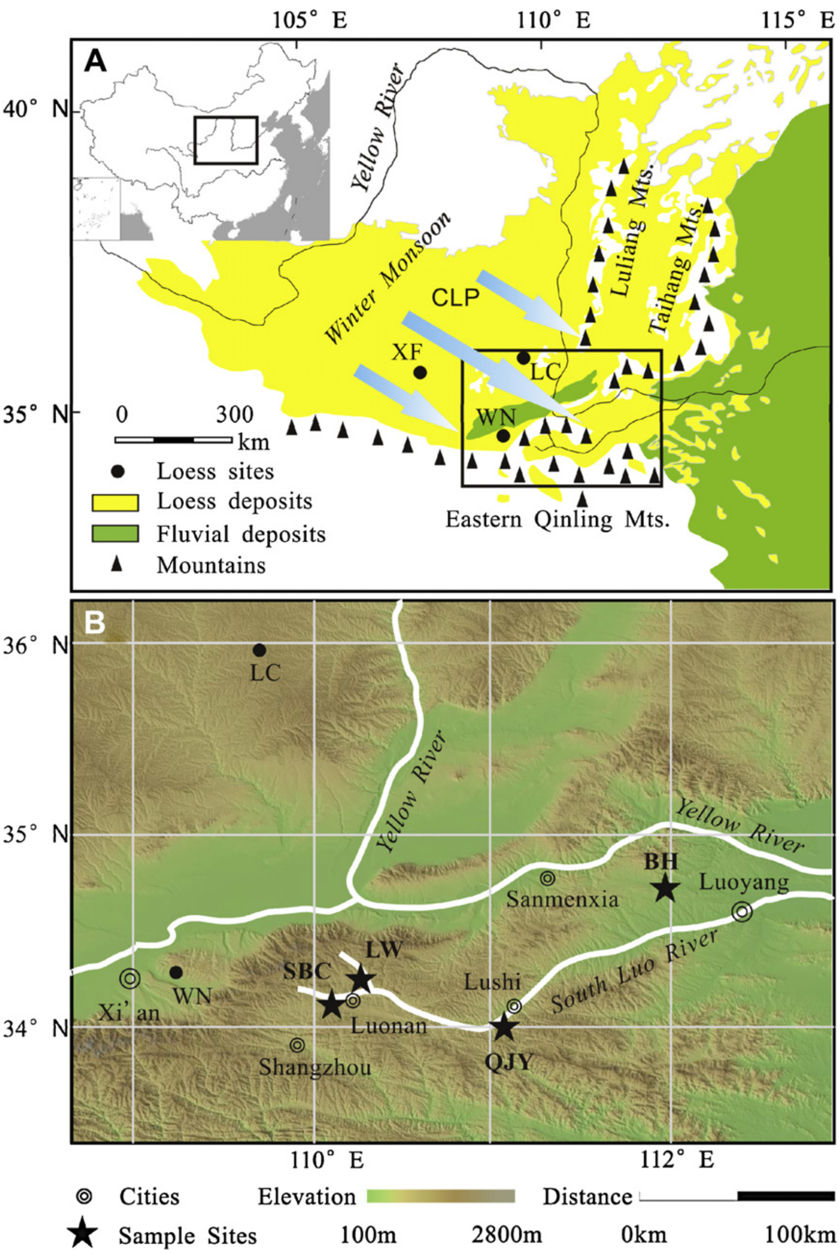

Fig. 1. A schematic map of loess distribution and sites studied and mentioned in this paper. A: the Chinese Loess Plateau (CLP) (modified from the National Atlas Editorial Board of China, 1999); B: loess sections at the Eastern Qinling Mountains (DEM date from http://srtm.csi.cgiar.org/). Stars indicate sampling sites (SBC: Shangbaichuan; LW: Liuwan; QJY: Qiaojiayao; BH: Baohou) and points are the sites mentioned (LC: Luochuan; XF: Xifeng; WN: Weinan).

revealed a better understanding of the behaviour of monsoon circulation at this environmental boundary.

The loess in the EQLM has previously been suggested to be of a periglacial (Wang, 1984) or desert origin (Lei, 1998). In recent years, a chronology of the loess-paleosol sequences has been established (Lu et al., 2007, 2011a,b) while grain size distribution (Zhang et al., 2008), magnetic properties (Zhao et al., 2008) and the soil organic carbon isotopic composition (Zhang et al., 2009) has also been investigated. However, dust provenance and its transport mechanism remain largely unclear.

The EQLM region is also regarded as an ideal place for early Pleistocene human settlement, with more than 13,500 Paleolithic artifacts discovered in the loess deposits (Wang, 2005; Shaanxi Provincial Institute of Archaeology, 2007; Wang et al., 2008a,b). Thus, a full understanding of the deposition and formation of the loess is needed before interpreting the paleoenvironmental record that formed the climatic backdrop to hominine occupation.

The purpose of this study is to investigate the provenance of these loess deposits, using multidisciplinary methods such as an analysis of landforms and atmospheric circulation, depositional environments, geochemical and strontium (Sr)/neodymium (Nd) isotopic compositions. The results of these analyses assist in understanding the paleoenvironment during the early human colonisation.

2. Geology and geographical setting

The Qinling Mountains is located on a structural belt between the North China Plate and the Yangtze Plate. The Qinling orogen was formed by collisions of these intra-continental plates during the Mesozoic era (e.g. Zhang et al., 1996; Wang et al., 2004). It stretches for over 2000 km in an east-west direction, with an average elevation between 1500 and 2500 m (Fig. 1B).

The South Luo River originates from the southern slope of Huashan Mountain in the middle of the QMB; it flows through the Luonan, Lushi and Luoning Basins, finally joining the Yellow River (the second largest river in China) at Luoyang (Fig. 1A, B). Landforms along this river are middle altitude mountains, basins and river terraces which are covered with up to tens metres of loess. The vegetation consists of subtropical broad-needle leaf mixed forest and grass. The annual temperature is 14.9 °C in lower reaches, 12.5 °C in middle reaches and 11.0 °C in the upper reaches along the river. The annual precipitation is 578.2 mm, 622.3 mm and 705.8 mm, respectively. The Asian Monsoon circulation mainly controls the rainfall.

3. Materials and methods

After intensive field reconnaissance, we identified and investigated four representative loess sections in the EQLM (Fig. 1B). The Shangbaichuan (SBC, 34°04′03″N, 110°03′06″E, 1037 m elevation, 25 m thick) and the Liuwan (LW, 34°08′37″N, 110°08′13″E, 948 m elevation, 13 m thick) sections are located in the Luonan Basin. The Qiaojiayao section (QJY, 33°59′36″N, 110°59′36″E, 611 m elevation, 19.7 m thick) is located in the Lushi Basin in its middle reaches, and the Baohou section (BH, 34°44′52.6″N, 111°57′53.7″E, 295 m elevation, 6.5 m thick) is located on a piedmont plain in the lower reaches of the South Luo River.

Sixteen samples from the SBC and LW sections were collected, pretreated with acid leaching to exclude effects of pedogenesis and carbonate (Chen et al., 2001; Yang et al., 2009) and analyzed for major elements using X-ray fluorescence (XRF) spectrometry. Trace element abundance that included rare earth element (REE) content from 12 bulk samples were measured according to the stratigraphic levels (Lu et al., 2007) by an inductively coupled plasma-mass spectrometer (ICP-MS) with indium (In) as an internal standard. One sample (LW1230) from the bottom of the LW section represented loess mixed with fluvial sediments.

Fifteen samples were measured for the Sr and Nd isotopic composition. The Sr–Nd isotopic ratios of acid-insoluble residues of the bulk samples were determined by thermal ionization mass spectrometry (TIMS) following the method of Chen et al. (2007). Reproducibility and accuracy were checked by running the strontium standard NIST SRM 987 and neodymium standard JNdi-1, with a mean of $^{87}Sr/^{86}Sr$ of 0.710248 ± 0.000005 (external $\pm 2\sigma$, $n = 12$) and $^{143}Nd/^{144}Nd$ of 0.512120 ± 0.000008 (external $\pm 2\sigma$, $n = 12$), respectively. Grain-size of these 15 samples was also measured using a Malvern Mastersizer S Laser diffraction particle analyzer and was pretreated using the method of Lu and An (1997).

All the samples were named as abbreviation of the section following by the sampling level (cm). For example, the sample LW20 was taken from the Liuwan loess section at depth of 20 cm.

4. Results and discussion

4.1. Loess distribution

The loess in the catchment of the South Luo River is distributed on various landforms at various heights. It is deposited in inter-mountain basins and on river terraces, with a thickness of several tens of meters, while in contrast, the loess on mountains tops or high reliefs are always several meters thick. The highest loess found is at an altitude of 1211 m in this catchment. In the western part of this region, relatively thin loess (less than 25 m) is deposited (Fig. 2A, B). The loess deposit gradually thickens along the river to the east to a depth of over 90 m. A loess tableland has formed in the middle of the river catchment.

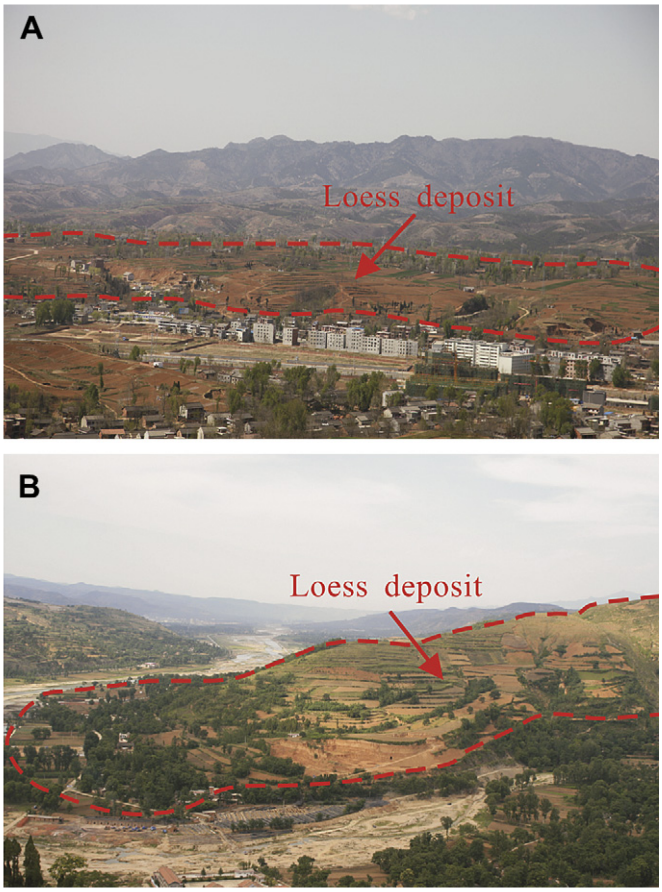

Fig. 2. Loess deposits along the South Luo River in the Eastern Qinling Mountains. A: loess deposits in Luonan Basin, the upper reaches; B: loess deposits in the middle reaches, Lushi Basin.

Our field observations demonstrate that the loess and paleosols in the Luonan Basin were strongly weathered compared to the CLP. The loess units have a light brown (7.5YR 5/6) to light reddish-brown (7.5YR 5/8) colour and are usually thinner than the paleosol units, which have a reddish-brown (5YR 4/6) to dark reddish-brown (5YR 3/6) colour. The loess samples from the Luonan Basin are generally harder than those from the CLP, with abundance of reddish-brown ferric oxide films and black manganese oxide films or spots. In some levels of the loess-paleosol sequence, grey-yellow to light olive-green colours are present, indicating that they developed in a reductive environment. Most of the paleosols have a block structure with conspicuous perpendicular cracks. The pH values of the loess from the Luonan Basin are between 6.0 and 7.0, suggesting weakly acid soil conditions. There was no reaction with dilute hydrochloric acid and no calcium carbonate cores or calcium films were observed. Compared with the loess on the CLP, there are no distinct differences between the paleosol and loess in the EQLM. This evidence indicates that the loess of the EQLM may be of wind-blown origin and has suffered relatively strong weathering.

4.2. The synoptic analysis of dust transport

When dust is blown up from sediments in central Asia and north China, the westerlies in the Northern Hemisphere transport this dust to the north Pacific Ocean, and form a latitudinal belt of quartz-rich sediments at about 30–40°N (Rex and Goldberg, 1958;

Rea, 1994; Vandenberghe et al., 2006). The low-altitude wind of the East Asian winter monsoon carries dust southeastward to the CLP (Liu, 1985; Liu and Ding, 1998; Lu and Sun, 2000; Nugteren and Vandenberghe, 2004; Yang et al., 2007a, 2008, 2011). When dust flows over the EQLM, the mountains probably block the coarser particles, suspended at lower elevations, while the fine particles (mostly <20 μm), suspended at higher levels cross over the mountains to be deposited in the intermountain basins in the EQLM. At low levels, the northwestern wind is disturbed by topography and a local wind circulation develops, with stronger winds forming at the mouth of the valleys (Scorer, 1952). This strengthened local wind probably blew fine particles into the mountain entrance and mixed them with the high-level dust from northern China. This process may have caused the varied composition of the loess at the EQLM, derived from both local and regional sources.

In addition, some dust transported by the westerlies may have also mixed with the loess deposit at the EQLM. However, it is probable that the Eastern Asian winter monsoon and the local wind are the dominant agents in dust transportation and deposition. This is because deposition by the westerlies occurs over very large regions and at very low sedimentation rates in north China, although the westerlies could raise dust to an altitude over 3000 m (Pye, 1987; Liu and Ding, 1998; Prins et al., 2007). Thus, the westerly-bearing dust only makes a small contribution to the loess along the South Luo River and is very difficult to identify. In addition, we have not seen any loess on elevations above 2000 m in the Qinling Mountains.

While we were in the field on April 30th, 2011, we observed a dust storm in the Luonan Basin. The dark sky indicated that dust was suspended in the wind with sediments eventually settling as a film on tables, cars and roof surfaces. Data from the China Meteorological Administration show the progress and direction of the dust storm (Fig. 3). This modern observation may confirm the aeolian origin of the loess at the EQLM and strengthen the argument for a dust source in northern China.

4.3. Grain-size distribution

Results of grain-size analysis show that the mean grain-size of the SBC and LW loess varies between 10 and 20 μm, most of the EQLM loess has a modal size (the size of the most frequent particles in grain-size distribution of a sample) of about 10 μm (Fig. 4). The amount of >63 μm fraction considered to be transported by rolling and saltation is very limited (<1%) and the <20 μm fraction is the principal constituent (60–90%). The grain-size has been used as an indicator of the distance from dust sources and its deposition areas. The fine fraction has been considered as an indicator for transport by the high-level westerly circulation. However, observations of modern dust storm deposits shows that fine grain-size is not necessarily related to high-level transportation processes because fine particles can form aggregates or adhere to larger grains during these storms (Qiang et al., 2010). Numerical simulations (Qin et al., 2005) suggested that the grain-size distribution in the loess-palaeosol sequence is largely dependent on near-surface wind strength during colder epochs rather than source distance. Therefore, the fine particles in LW and SBC sites may due to that transport agents were weak and/or the strongly weathering processes.

4.4. Major element contents

Analysis of major and trace elements in chemically insoluble residues is a useful technique for understanding origin and provenance of clastic sediments (Taylor and McLennan, 1985; McLennan et al., 1993). This approach has been widely used in provenance identification of aeolian deposits in various regions (Reheis et al., 2002; Sun, 2002; Yang et al., 2007a,b, 2008; Guan et al., 2008; Muhs et al., 2008; Bokhorst et al., 2009; Hao et al., 2010; Buggle et al., 2011; Qiao et al., 2011). The major elements that compose the EQL loess deposit are shown in Table 1. Loss on ignition (LOI), which reflects amounts of variable carbonates, clay minerals and organic matter in most samples, varies in a narrow range between 6.07% and 6.96%. This value is relatively higher than the Luochuan (LC) loess in the central CLP (4.43%–6.72%; Chen et al., 2001). Since acid pretreatment is used that has already dissolved carbonates, we considered that the high LOI might result from higher amounts of clay minerals and organic matter in the samples. Nevertheless, relatively low LOI values of 4.47% and 4.69% also occurred in two samples (LW575 and

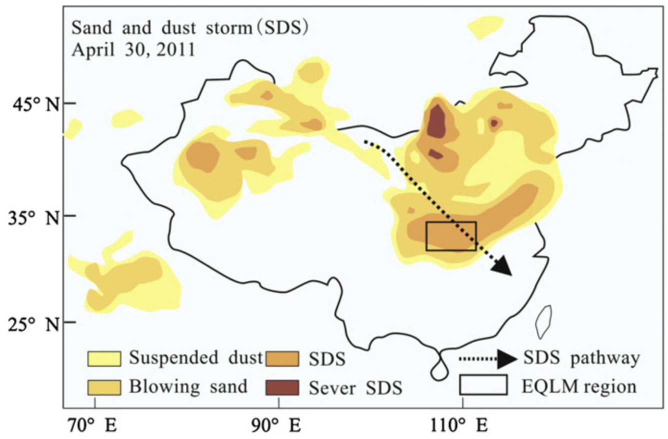

Fig. 3. A sand and dust storm (SDS) was observed in the Eastern Qinling Mountains during our field work (April 29 to May 1, 2011), supported by the numerical simulation (Centre for atmosphere watch and services, China, www.sds.cma.gov.cn), indicating the SDS floating in the EQLM at 6:00 AM, April 30, 2011.

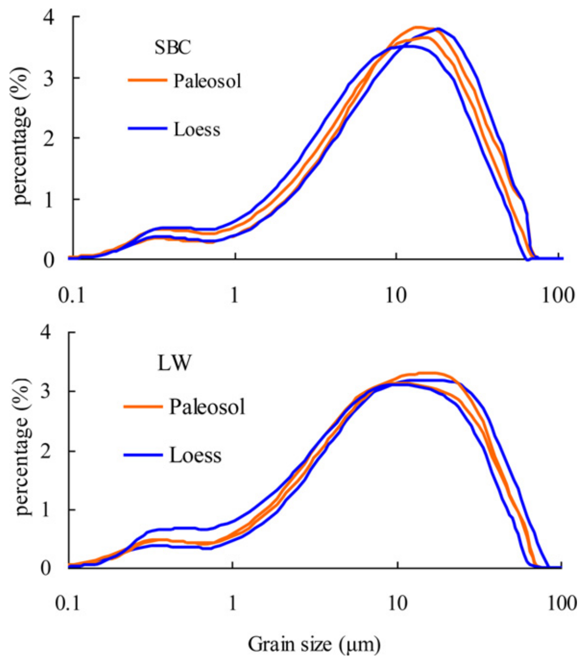

Fig. 4. Grain-size distribution of the loess samples from the Eastern Qinling Mountains (for locations, see Fig. 1B).

Table 1
Mean concentrations (wt %) of major elements of loess from the Eastern Qinling Mountains (for locations see Fig. 1B).

Sample	Fe_2O_3	MnO	TiO_2	SiO_2	Al_2O_3	K_2O	MgO	Na_2O	CaO	P_2O_5	LIO	SUM
LW20	6.13	0.09	0.79	65.12	15.05	2.52	1.60	1.37	0.65	0.09	6.64	100.05
LW140	6.27	0.11	0.79	64.69	15.35	2.75	1.74	1.47	0.79	0.12	6.07	100.15
LW290	6.11	0.09	0.84	65.55	15.20	2.53	1.40	1.22	0.56	0.08	6.35	99.93
LW285	6.11	0.12	0.84	65.62	15.08	2.56	1.42	1.22	0.58	0.08	6.26	99.90
LW575	6.03	0.07	0.88	68.41	14.48	2.52	1.30	1.29	0.60	0.11	4.47	100.15
LW1000	6.18	0.09	0.76	64.35	15.62	2.73	1.57	1.33	0.66	0.10	6.52	99.93
LW1230	5.84	0.14	0.84	70.90	12.36	2.86	1.11	0.60	0.38	0.10	4.69	99.82
SBC25	6.38	0.10	0.77	64.20	15.61	2.55	1.68	1.34	0.70	0.06	6.77	100.15
SBC140	6.50	0.09	0.79	64.04	15.86	2.64	1.64	1.29	0.68	0.10	6.69	100.33
SBC390	6.16	0.10	0.85	65.42	15.47	2.45	1.36	1.06	0.54	0.05	6.64	100.11
SBC635	6.59	0.11	0.86	64.71	15.36	2.51	1.44	1.22	0.64	0.11	6.64	100.18
SBC785	6.44	0.07	0.77	64.17	15.62	2.64	1.62	1.31	0.71	0.10	6.89	100.33
SBC945	6.47	0.16	0.82	63.65	15.74	2.79	1.64	1.31	0.75	0.15	6.68	100.16
SBC1380	6.55	0.10	0.78	63.83	15.63	2.77	1.64	1.32	0.74	0.14	6.80	100.30
SBC1930	5.66	0.12	0.86	66.79	14.92	2.54	1.34	1.06	0.58	0.09	6.29	100.26
SBC2320	6.38	0.09	0.76	64.05	15.53	2.80	1.64	1.28	0.75	0.11	6.96	100.35

LW1230). Based on the field observation, strong weathering and leaching may have modified these sediments.

In the UCC-normalized spider diagrams of the major elements (Taylor and McLennan, 1985), the SBC and LW loess display a similar pattern to that of typical LC loess (Chen et al., 2001) (Fig. 5). Distribution of the major elements in all the samples from SBC and LW sites are similar and conform well to those of the typical loess, indicating the loess at the EQLM has experienced multiple recycling and were well mixed. Compared with the UCC, the diffluent elements such as Na are strongly diluted and immobile elements such as Si, Al and Ti are relatively stable. This characteristic supports observations by Chen et al. (2001) that the loess was exposed at the surface and consequently experienced a certain degree of weathering. Compared with LC loess values, the Ca, Na and P in the SBC and LW samples show a greater degree of depletion. For example, the mole ratio of CaO/Al_2O_3 in the loess at the EQLM ranges from 0.06 to 0.09 and Na_2O/Al_2O_3 ranges from 0.08 to 0.16, which is significantly lower than those rations in the LC loess (0.07–0.16 and 0.14 to 0.24, respectively). Moreover, K and Mg, which are slightly more stable than Ca and Na, began diluting in the SBC and LW loess, suggesting that the dissolution of detrital minerals has transformed from the plagioclase-destruction phase (primary weathering phase) to the potassium feldspar-destruction phase (moderate weathering phase). The Chemical Index of Alteration [$CIA = Al_2O_3/(Al_2O_3 + CaO^* + Na_2O + K_2O) \times 100$, all refer to the mole fraction. CaO^* represents the Ca in silicate fraction only] was widely used as an indicator of chemical weathering, and varies between 69 and 74 in the studied loess. It is higher than the LC loess, which ranges between 61 and 69, suggesting the loess has suffered from stronger weathering than that in the central Chinese Loess Plateau. We also use the Chemical Proxy of Alteration ($CPA = 100 \times Al_2O_3/(Al_2O_3 + Na_2O)$ in molar proportions) which was recommended by Buggle et al. (2011). The results show that the CPA and CIA show a similar behaviour in all measured samples except the relatively higher CPA value in LW1230 due to the exclusion effect of K fixation on clay minerals (Nesbitt and Young, 1984, 1989; Yang et al., 2004). The relative enrichment of Fe and Mn is consistent with the occurrence of abundant Fe–Mn and clay mineral films observed in the field, indicating an intense pedogenesis.

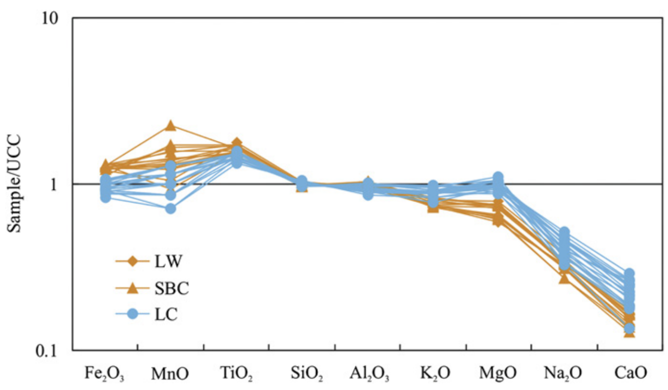

Fig. 5. The UCC-normalized spider diagrams of the major element (for locations see Fig. 1A, B). Data of the Luochuan loess (LC) from Chen et al. (2001); The UCC data from Taylor and McLennan (1985).

4.5. *Trace and rare earth element concentrations*

The trace and rare earth element (REE) concentrations and patterns are useful tools to investigate loess provenance (López et al., 2005; Yang et al., 2007b). Our results are shown in Table 2. Fig. 6A shows the Chondrite-normalized REE distribution patterns, while Fig. 6B shows the selected trace element UCC-normalized spider diagram. Both are compared with that of the typical loess in Xifeng (XF) on the CLP (Jahn et al., 2001). The concentrations of the trace and rare earth elements are rather uniform in the SBC and LW loess, and the two sites show trace element distributions that are very similar to those of the XF loess, being close to the UCC trace element composition. The Chondrite-normalized REE distribution patterns of both the SBC and LW loess are characterized by steep light-REE (LREE) and relatively flat heavy-REE (HREE) curves with negative Eu anomalies. These REE distribution features are identical to those of UCC and the CLP loess, which provide further evidence that the loess at the EQLM has been relatively well mixed. The Ba/Sr molar ratio is considered to be controlled by the weathering intensity and leaching intensity (Gallet et al., 1996; Bokhorst et al., 2009). The Ba/Sr ratios in the LW and SBC loess range between 3.26 and 4.32, which are distinctly larger than that in XF, these are between 1.33 and 1.89 (Jahn et al., 2001), indicating that the EQLM loess may have experienced more intensive weathering and leaching.

Nevertheless, some differences occur between the loess in the EQLM and the CLP loess. The SBC and LW loess have a higher concentration in most of the trace elements, except for a clear depletion in Sr, including higher $\sum$REE than the XF loess. This is because trace elements tend to be enriched in fine particles and the strong weathering processes concentrate these stable elements to a certain extent (López et al., 2005; Yang et al., 2007b).

Table 2
Mean concentrations (μg/g) of trace elements of loess from the Eastern Qinling Mountains (for locations see Fig. 1B).

Sample	LW20	LW140	LW575	LW1000	LW1230	SBC25	SBC140	SBC635	SBC785	SBC945	SBC1380	SBC2320
V	135	137	146	143	126	141	148	152	140	149	160	140
Cr	117	143	119	133	123	99	118	166	125	122	129	212
Co	17.1	18.5	22.2	14.8	21.6	16.8	17.0	18.5	13.1	23.7	15.7	14.8
Ni	54.5	68.6	43.3	49.9	41.5	38.8	57.8	56.6	38.9	67.8	51.8	65.1
Cu	25.5	29.0	21.0	29.1	22.9	27.2	29.9	24.5	26.7	33.4	33.7	26.8
Zn	74.2	71.4	65.7	82.8	66.6	61.6	76.2	73.0	73.2	88.4	79.0	75.0
Rb	136	149	149	145	134	132	149	158	146	151	146	156
Sr	107	118	124	118	119	109	136	122	117	128	118	110
Y	34.5	39.1	35.2	38.9	33.3	32.4	42.0	38.4	37.1	41.1	40.8	36.6
Zr	327	288	327	284	353	302	436	329	271	263	300	328
Nb	17.4	17.8	20.6	17.0	18.4	17.3	19.4	19.6	17.6	19.0	18.0	20.3
Cs	11.3	11.8	10.6	10.8	8.8	11.2	12.3	14.6	12.8	11.9	12.6	13.5
Ba	601	635	645	796	719	614	805	627	599	666	615	624
La	45.5	48.4	47.9	55.2	53.1	44.6	51.8	51.6	48.2	49.3	46.6	48.7
Ce	91.4	99.1	92.9	95.2	128.7	100.3	95.9	109.6	98.1	106.8	90.3	98.5
Pr	10.3	10.9	11.1	12.1	11.8	10.4	11.9	11.6	10.9	11.7	10.6	11.2
Nd	38.8	41.8	40.4	45.9	43.5	38.8	43.7	42.3	41.7	43.3	41.6	41.3
Sm	7.15	7.65	7.46	8.39	7.42	7.00	8.12	8.07	7.96	8.31	7.86	7.39
Eu	1.48	1.66	1.52	1.74	1.58	1.55	1.70	1.68	1.67	1.74	1.62	1.50
Gd	6.55	6.86	6.55	7.81	6.04	6.19	7.54	7.16	7.11	7.46	7.12	6.60
Tb	0.91	0.95	0.90	1.06	0.82	0.87	1.03	0.95	0.94	0.99	0.97	0.87
Dy	6.22	6.40	6.42	7.12	5.62	5.95	6.85	6.72	6.45	7.15	6.92	6.08
Ho	1.31	1.42	1.35	1.53	1.26	1.31	1.52	1.40	1.41	1.49	1.55	1.34
Er	4.13	4.76	4.36	4.36	3.76	3.80	4.49	6.43	5.58	4.50	5.12	5.73
Tm	0.56	0.58	0.61	0.62	0.53	0.57	0.65	0.59	0.59	0.64	0.64	0.57
Yb	3.47	3.62	3.66	3.91	3.29	3.47	3.93	3.67	3.68	3.89	4.13	3.50
Lu	0.55	0.58	0.58	0.61	0.50	0.54	0.64	0.58	0.56	0.61	0.65	0.57
Hf	8.58	7.57	8.44	7.93	8.43	7.89	9.08	8.34	7.36	7.10	7.92	8.33
Ta	1.34	1.39	1.53	1.27	1.33	1.36	1.44	1.46	1.35	1.45	1.35	1.55
Pb	24.1	23.2	28.1	20.9	35.4	23.7	23.0	28.2	21.6	24.9	21.9	21.1
Th	16.9	15.5	17.7	16.1	14.5	16.5	18.2	17.5	17.2	17.4	17.0	17.6
U	3.38	3.19	3.84	3.43	3.32	3.52	3.58	3.66	3.28	3.53	3.55	3.60

4.6. Sr–Nd isotopic compositions

The Sr and Nd isotopic compositions have long been considered as useful indicators for dust provenance (e.g., Grousset and Biscaye, 2005; Chen and Li, 2011). The reason is that the $^{87}Sr/^{86}Sr$ and $^{143}Nd/^{144}Nd$ ratios of the sediments are variable depending on their origins and ages, and these isotopic ratios remain largely unchanged during transportation, deposition and weathering (Grousset and Biscaye, 2005). Therefore, the Sr–Nd isotopic ratios have been widely used as sensitive tracers for provenance of the loess deposit (Liu et al., 1994; Gallet et al., 1998; Jahn et al., 2001; Chen et al., 2007; Li G.J. et al., 2009). Systematic investigation of silicate Sr–Nd isotopic compositions (Chen et al., 2007) indicates that the Sr–Nd isotopic signature of the CLP loess and fine fractions (<75 μm) of the potential dust sources in China could have remained relatively stable over the past million years.

Silicate Sr and Nd isotopic compositions of samples from the SBC, LW, QJY and BH sections and their correlative stratigraphic positions are given in Table 3. Comparison between the Sr–Nd isotopic composition of the loess at the EQLM and the CLP loess (Li G.J. et al., 2009) and the isotope values of three major potential dust sources (Chen et al., 2007; Li G.J. et al., 2009) are shown in Fig. 7. The $\varepsilon_{Nd}(0)$ values of loess from the EQLM have a large range between −11.98 and −18.97, with an average of −14.98. The $^{87}Sr/^{86}Sr$ ratios are relatively uniform, showing a small variation between 0.719650 and 0.721043, with an average of 0.720294. These Sr–Nd isotope data imply: 1) loess from both central and south of the CLP have roughly identical Sr–Nd isotopic composition, but that of the EQLM loess scattered in a large range, distinctly different from that of the CLP loess. 2) The Sr–Nd isotope data of the CLP loess fall in the range of the northern margin of the Tibetan Plateau (NMTP), which belongs to the younger upper crust range. In

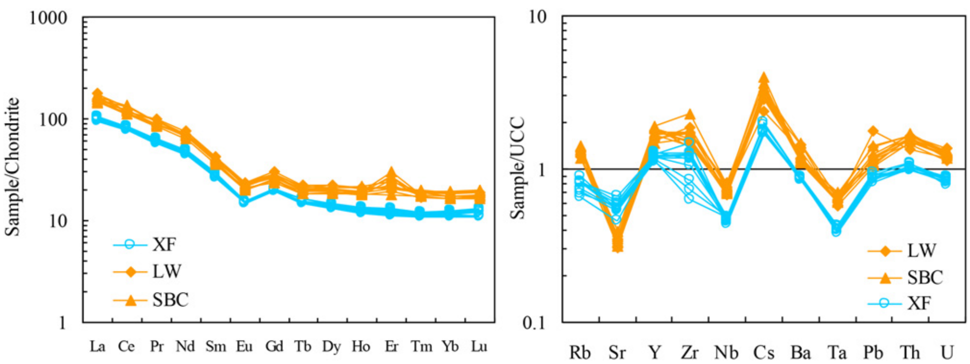

Fig. 6. Chondrite-normalized REE distribution patterns for loess samples (left) and the UCC-normalized spider diagrams of the trace element (right) (for locations see Fig. 1A, B). Data for Xifeng loess (XF) from Jahn et al. (2001); The UCC data from Taylor and McLennan (1985); Chondrite values used are from Boynton (1984).

Table 3
Sr and Nd isotopic compositions of loess and paleosol samples from eastern Qinling Mountains (for locations see Fig. 1B).

Sample	Loess/Paleosol	$^{87}Sr/^{86}Sr$	2σ	$^{143}Nd/^{144}Nd$	2σ	$\varepsilon_{Nd}(0)$[a]
LW130	Loess	0.719935	0.000012	0.511665	0.000012	−18.97
LW340	Paleosol	0.720577	0.000002	0.512024	0.000003	−11.98
LW640	Paleosol	0.720136	0.000012	0.511836	0.000006	−15.65
LW830	Loess	0.720345	0.000019	0.511952	0.000005	−13.39
SBC50	Paleosol	0.719979	0.000002	0.511905	0.000006	−14.30
SBC450	Loess	0.720641	0.000010	0.511744	0.000010	−17.44
SBC550	Paleosol	0.719650	0.000038	0.511700	0.000012	−18.29
SBC1650	Loess	0.720342	0.000005	0.511993	0.000004	−12.57
SBC2250	Loess	0.721043	0.000003	0.512013	0.000004	−12.19
QJY200	Paleosol	0.719995	0.000010	0.511558	0.000018	−21.07
QJY400	Loess	0.719562	0.000002	0.511796	0.000006	−16.42
QJY600	Loess	0.719554	0.000002	0.511118	0.000014	−29.66
QJY1000	Paleosol	0.719842	0.000003	0.511476	0.000010	−22.67
BH150	Loess	0.718807	0.000003	0.511619	0.000006	−19.88
BH500	Paleosol	0.719614	0.000009	0.511638	0.000005	−19.51

[a] $\varepsilon_{Nd}(0) = [(^{143}Nd/^{144}Nd)_{sample}/(^{143}Nd/^{144}Nd)_{CHUR} - 1] \times 10000$; $(^{143}Nd/^{144}Nd)_{CHUR} = 0.512638$.

contrast, only part of the loess at the EQLM falls in the NMTP range, and most of the Sr–Nd isotope data of this loess are different from the corresponding values of the three potential dust sources. The relatively higher $^{87}Sr/^{86}Sr$ ratios and the extremely low $\varepsilon_{Nd}(0)$ values, which distinctly exceed the range of the younger upper crust, obviously indicate that the EQLM loess probably has at least mixed sources. One source is the same as for the CLP loess; the other one may be nearby bedrock of the Qinling orogen belt, representing materials initially from the old crust.

Previous studies have demonstrated that the dust sources of Chinese loess are strongly related to tectonic belts and mountain ridges (Chen et al., 2007; Stevens et al., 2010). The North China Plate at the north side of the Qinling Mountains is one of the oldest and most stable cratons in China (Zhang et al., 1996). Sediments derived from this old continental shield can produce low $\varepsilon_{Nd}(0)$ values and high $^{87}Sr/^{86}Sr$ ratios. A systematic isotope study showed that the granite and clastic bedrock in the south of the North China Plate and the Qinling orogen belt have very low $\varepsilon_{Nd}(0)$ and high $^{87}Sr/^{86}Sr$ ratios (Zhang et al., 2006). Thus, the Sr–Nd isotope signature of the loess samples from the middle and lower reaches of the South Luo River with high $^{87}Sr/^{86}Sr$ ratios and even more negative $\varepsilon_{Nd}(0)$ values (Table 3) reveal that a local source has significantly contributed to this loess.

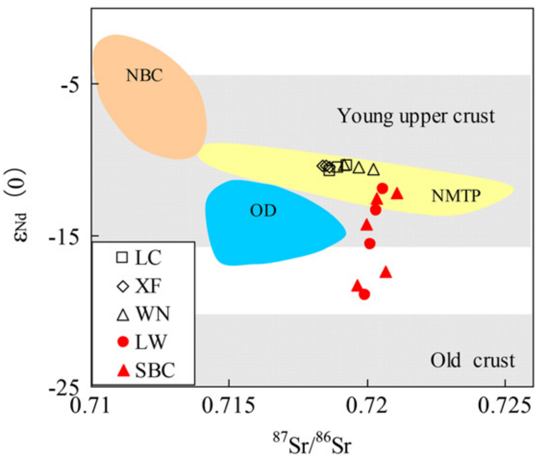

Fig. 7. Sr–Nd isotopic compositions of loess in the Eastern Qinling Mountains. Isotopic compositions of the potential sources of Asian dust and the CLP loess from Chen et al. (2007) and Li G.J. et al., 2009. NBC: the deserts around northern boundary of China; NMTP: the arid lands of the northern margin of Tibetan Plateau; OD: the Ordos Desert (for locations, see Fig. 1A, B).

4.7. Contribution of potential multiple dust sources

The Sr–Nd isotopic ratios of the loess samples from the EQLM and its eastern pediment plain are distinctly different from that of the potential dust sources of the CLP loess. The Sr–Nd isotopic ratios also show that the dust sources may have changed both temporally and spatially. These data suggest that local dust is a major contributor. Similarly, studies of the Mangshan loess near Sanmenxia (Fig. 1) suggested a source either derived from fluvial sediments of the Yellow River or from the ancient alluvial fan lying at the eastern end of the Sanmen Gorge (Jiang et al., 2007; Zheng et al., 2007) has significantly contributed to the loess deposit. This may provide an analogue that the local sources have contributed substantially to the loess deposition in our study region. However, as indicated by the modern dust storm pathways, dust from the northern and northwestern China may provides another potential dust source.

4.8. The paleoenvironmental implications

The distribution of loess has been used previously to argue that the climate was relatively cold and dry at both its source and deposition points (Liu, 1985; Liu and Ding, 1998). However, other researchers have proposed that the climatic conditions leading to loess deposition in northwestern China do not necessarily represent palaeo-environments elsewhere. On-site evidence is crucial in understanding the varied environmental conditions across China at these times (Yang and Scuderi, 2010; Yang et al., 2011). We have shown that the intermountain basins in the EQLM had a relatively warm and humid climate during glacial periods, compared with their counterparts in the central Chinese Loess Plateau which is evidenced by strongly developed paleosols, heavy chemical weathering, and higher clay content. Field investigations also suggest that there are more Fe–Mn bands and spots in the paleosols and loess units in the EQLM when compared to the CLP paleosols and loess. These are indicative of stronger weathering in the EQLM.

Palynological data (Lei, 2000) obtained from a loess-paleosol section near the Luonan Basin show that pollen grains from woody species are relatively richer compared with those of the CLP. The high proportions of *Quercus* and *Castanea* indicate warm-temperate forest vegetation that reflects an optimum climate when the paleosol developed. In the loess units, the increase of herbaceous species indicates a relative decline in annual temperature and rainfall in comparison with the paleosols. However, the existence of trees like *Betula* and *Pinus* and, herbs like *Cyperaceae* and *Typha* in the loess units demonstrate that the climate was cool and remained humid even in the glacial period. Organic carbon isotopic analysis of the SBC and LW loess (Zhang et al., 2009) shows similar results as those of the pollen analysis, revealing that the C_3 plants (trees) dominated the vegetation mix of C_3 and C_4 plants (grasses) in the Luonan Basin, while C_4 grasses mainly covered the central Chinese Loess Plateau at the same time (Zhang et al., 2003).

Investigations of the loess stratigraphy and the associated Paleolithic archaeological sites show that early humans occupied the Luonan Basin from at least 0.80–0.70 Ma (Lu et al., 2007, 2011a). Sites have also been found in the Lushi Basin dating to 0.62–0.60 Ma (Lu et al., 2011b) while hundreds of artifacts have been found in the loess with an age of 0.40–0.30 Ma and 0.20–0.10 Ma (Lu et al., 2011a). Over 13,500 Paleolithic stone artifacts have been collected from 268 open-air localities in the Luonan Basin (Wang, 2005; Shaanxi Provincial Institute of Archaeology, 2007; Wang et al., 2008a), and many originate from loess deposits. The high number of archaeological sites in the EQLM dating to the middle Pleistocene suggest that despite the cold climatic conditions in northern China, a more attractive environment existed in the EQLM for the early human occupation than on the CLP. The loess deposits thus provide valuable archives to understand age, environment and landform from the period when our human ancestors lived in this region.

5. Conclusions

Loess in the EQLM has two mixed sources, with one derived from the local clastic deposits produced from the weathered bedrock of the proximal orogen belt and adjacent alluvial–fluvial sediments. The other one originates from the deserts, piedmont alluvial fans and dryland in northern and northwestern China. The eastern Asian winter monsoon and local wind are the major atmospheric circulations transporting the dust deposited in the EQLM. The loess suffered a stronger weathering than the loess in the central Chinese Loess Plateau, principally because of the warm and humid climate during the middle Pleistocene. These milder climatic conditions were attractive to early human populations, thus the archaeological evidence distributed widely in the Luonan Basin and elsewhere in this region.

Acknowledgements

We thank Cunfa Zhao, Jun Zhao, Xuefeng Sun, Xianyan Wang, Xiaoyong Wang, Xiaobing Zhang, Ming Wei, Chen Shen, Wenchao Zhang, Zhimin Qiu, Langping Li, Yingyong Chen and Yali Zhou for their helps in the fieldworks. Thanks also go to Shuangwen Yi, Chuanbin Yang, Wei Pu, Weihua Wu, Lianwen Liu and Huimin Li for their helps for the laboratory work. This study was supported by the National Natural Science Foundation of China (40930103, 41072122, and 41021002); the Scientific Research Foundation of Graduate School of Nanjing University (2010CL08); the 100 Talents Program of Chinese Academy of Sciences (KZCX2-YW-BR-24) and the Australia Research Council (DP0665250).

References

Bokhorst, M.P., Beets, C.J., Markovic, S.B., Gerasimenko, N.P., Matviishina, Z.N., Frechen, M., 2009. Pedo-chemical climate proxies in Late Pleistocene Serbian–Ukrainian loess sequences. Quaternary International 198, 113–123.

Boynton, W.V., 1984. Cosmochemistry of the rare earth elements: meteorite studies. In: Henderson, P. (Ed.), Rare Earth Element Geochemistry. Elsevier, Amsterdam, pp. 63–114.

Buggle, B., Glaser, B., Hambach, U., Gerasimenko, N., Markovic, S., 2011. An evaluation of geochemical weathering indices in loess-paleosol studies. Quaternary International 240, 12–21.

Chen, J., An, Z.S., Liu, L.W., Ji, J.F., Yang, J.D., Chen, Y., 2001. Variations in chemical compositions of the eolian dust in Chinese Loess Plateau over the past 2.5 Ma and chemical weathering in the Asian inland. Science in China, Series D 44, 403–413.

Chen, J., Li, G.J., Yang, J.D., Rao, W.B., Lu, H.Y., Balsam, W., Sun, Y.B., Ji, J.F., 2007. Nd and Sr isotopic characteristics of Chinese deserts: implications for the provenances of Asian dust. Geochimica et Cosmochimica Acta 71, 3904–3914.

Chen, J., Li, G.J., 2011. Geochemical studies on the source region of Asian dust. Science in China: Earth Science 54, 1279–1301.

Gallet, S., Jahn, B., Torii, M., 1996. Geochemical characterization of the Luochuan loess paleosol sequence, China, and paleoclimatic implications. Chemical Geology 133, 67–88.

Gallet, S., Jahn, B.M., Lanoe, B.V.V., Dia, A., Rossello, E., 1998. Loess geochemistry and its implications for particle origin and composition of the upper continental crust. Earth and Planetary Science Letters 156, 157–172.

Grousset, F.E., Biscaye, P.E., 2005. Tracing dust sources and transport patterns using Sr, Nd and Pb isotopes. Chemical Geology 222, 149–167.

Guan, Q.Y., Pan, B.T., Gao, H.S., Li, N., Zhang, H., Wang, J.P., 2008. Geochemical evidence of the Chinese loess provenance during the Late Pleistocene. Palaeogeography, Palaeoclimatology, Palaeoecology 270, 53–58.

Guo, Z.T., Biscaye, P.E., Wei, L.Y., Chen, X.F., Peng, S.Z., Liu, T.S., 2000. Summer monsoon variations over the last 1.2 Ma from the weathering of loess-soil sequences in China. Geophysical Research Letters 27, 1751–1754.

Hao, Q.Z., Guo, Z.T., Qiao, Y.S., Xu, B., Oldfield, F., 2010. Geochemical evidence for the provenance of middle Pleistocene loess deposits in southern China. Quaternary Science Reviews 29, 3317–3326.

Jahn, B., Gallet, S., Han, J.M., 2001. Geochemistry of the Xining, Xifeng and Jixian sections, Loess Plateau of China: Eolian dust provenance and paleosol evolution during the last 140 ka. Chemical Geology 178, 71–94.

Jiang, F., Fu, J., Wang, S., Sun, D., Zhao, Z., 2007. Formation of the Yellow River, inferred from loess palaeosol sequence in Mangshan and lacustrine sediments in Sanmen Gorge, China. Quaternary International 175, 62–70.

Lei, X.Y., 1998. Grain size analysis and genesis of loess in the Qinling Mountains. Acta Geological Sinica 72, 178–188 (in Chinese, with English Abstr.).

Lei, X.Y., 2000. Vegetation and environment during period of loess-paleosol development in the Qinling Mountains. Marine Geology & Quaternary Geology 21, 73–79 (in Chinese, with English Abstr.).

Li, G.J., Chen, J., Ji, J.F., Yang, J.D., Conway, T.M., 2009. Natural and anthropogenic sources of East Asian dust. Geology 37, 727–730.

Li, X.S., Han, Z.Y., Chen, Y.Y., Cai, Y.F., Yang, D.Y., 2009. Characteristics and source of rain dust in Nanjing on March 11, 2006. Quaternary Sciences 29, 43–54 (in Chinese, with English Abstr.).

Liu, C.Q., Masuda, A., Okada, A., Yabuki, S., Fan, Z.L., 1994. Isotopic geochemistry of Quaternary deposits from the arid lands in northern China. Earth and Planetary Science Letters 127, 25–38.

Liu, T.S., 1985. Loess and the Environment. China Ocean Press, Beijing.

Liu, T.S., Ding, Z.L., 1998. Chinese loess and the paleomonsoon. Annual Reviews of Earth and Planetary Sciences 26, 111–145.

López, J.M., Bluluz, B., Yuste, A., Mayayo, M.J., Fernández-Nieto, C., 2005. Mineralogical and trace element composition of clay-sized fractions from Albian siliciclastic rocks (Oliete Basin, NE Spain). Clay Minerals 40, 565–580.

Lu, H.Y., An, Z.S., 1997. Pretreatment methods in loess-palaeosol granulometry. Chinese Science Bulletin 42, 237–240.

Lu, H.Y., Sun, D.H., 2000. Pathways of dust input to the Chinese Loess Plateau during the last glacial and interglacial periods. Catena 40, 251–261.

Lu, H.Y., Zhang, H.Y., Wang, S.J., Richard, C., Zhao, C.F., Thomas, S., Zhao, J., 2007. A preliminary survey on loess deposit in Eastern Qinling Mountains (central China) and its implication for estimating age of the Pleistocene lithic artifacts. Quaternary Science 27, 559–567 (in Chinese, with English Abstr.).

Lu, H.Y., Zhang, H.Y., Wang, S.J., Richard, C., Sun, X.F., Zhao, J., Sun, D.H., Zhao, C.F., Shen, C., Wei, M., 2011a. Multiphase timing of hominin occupations and the paleoenvironment in Luonan Basin, central China. Quaternary Research 76, 142–147.

Lu, H.Y., Sun, X.F., Wang, S.J., Richard, C., Zhang, H.Y., Yi, S.W., Ma, X.L., Wei, M., Yang, Z.Y., 2011b. Ages for hominin occupation in Lushi Basin, middle of South Luo River, central China. Journal of Human Evolution 60, 612–617.

McLennan, S.M., Hemming, S., McDaniel, D.K., Hanson, G.N., 1993. Geochemical approaches to sedimentation, provenance and tectonics. In: Johnsson, M.J., Basu, A. (Eds.), Processes Controlling the Composition of Clastic Sediments. Colorado, Boulder, pp. 21–40.

Muhs, D.R., Budahn, J.R., Johnson, D.L., Reheis, M., Beann, J., Skipp, G., Fisher, E., Jones, J.A., 2008. Geochemical evidence for airborne dust additions to soils in Channel Islands National Park, California. Geological Society of America Bulletin 120, 106–126.

National Atlas Editorial Board of China, 1999. The National Physical Atlas of China. China Maps Press, Beijing, 34 pp. (in Chinese).

Nesbitt, H.W., Young, G.M., 1984. Prediction of some weathering trends of plutonic and volcanic rocks based on thermodynamic and kinetic considerations. Geochimica et Cosmochimica Acta 48, 1523–1534.

Nesbitt, H.W., Young, G.M., 1989. Formation and diagenesis of weathering profiles. The Journal of Geology 97, 129–147.

Nugteren, G., Vandenberghe, J., 2004. Spatial climatic variability on the Central Loess Plateau (China) as recorded by grain size for the last 250 kyr. Global and Planetary Change 41, 185–206.

Prins, M.A., Vriend, M., Nugteren, G., Vandenberghe, J., Lu, H., Zheng, H., Weltje, G.J., 2007. Late Quaternary aeolian dust input variability on the Chinese Loess

Plateau: inferences from unmixing of loess grain-size records. Quaternary Science Reviews 26, 230–242.
Pye, K., 1987. Eolian Dust and Dust Deposits. Academic Press, London, 334 pp.
Qiao, Y.S., Hao, Q.Z., Peng, S.S., Wang, Y., Li, J.W., Liu, Z.X., 2011. Geochemical characteristics of the eolian deposits in southern China, and their implications for provenance and weathering intensity. Palaeogeography, Palaeoclimatology, Palaeoecology 308, 513–523.
Qiang, M., Lang, L., Wang, Z., 2010. Do fine-grained components of loess indicate westerlies: insights from observations of dust storm deposits at Lenghu (Qaidam Basin, China). Journal of Arid Environments 74, 1232–1239.
Qin, X.G., Cai, B.G., Liu, T.S., 2005. Loess record of the aerodynamic environment in the East Asia monsoon area since 60,000 years before present. Journal of Geophysical Research-Solid Earth 110, B01204.
Rea, D.K., 1994. The paleoclimatic record provided by eolian deposition in the deep sea: the geologic history of wind. Reviews of Geophysics 32, 159–195.
Reheis, M.C., Budahn, J.R., Lamothe, P.J., 2002. Geochemical evidence for diversity of dust sources in the southwestern United States. Geochimica et Cosmochimica Acta 66, 1569–1587.
Rex, R., Goldberg, E., 1958. Quartz contents of pelagic sediments of the Pacific Ocean. Tellus 10, 153.
Scorer, R.S., 1952. Mountain-gap winds; a study of the surface wind in Gibraltar. Quarterly Journal of the Royal Meteorological Society 78, 53–59.
Shaanxi Provincial Institute of Archaeology, Cultural Relics Administrative Committee of ShangluoDistrict, Museum of Luonan County, 2007. Huashilang (I): The Palaeolithic Open-air Sites in the Luonan Basin, China. Science Press, Beijing, 1–300 pp. (in Chinese, with English Abstr.).
Sun, J.M., 2002. Provenance of loess material and formation of loess deposits on the Chinese Loess Plateau. Earth and Planetary Science Letters 203, 845–859.
Stevens, T., Palk, C., Carter, A., Lu, H.Y., Clift, P., 2010. Assessing the provenance of loess and desert sediments in Northern China using U–Pb dating and morphology of detrital zircons. Geological Society of America Bulletin 122, 1331–1344.
Taylor, S.R., McLennan, S.M., 1985. The Continental Crust: Its Composition and Evolution. Blackwell, Oxford.
Vandenberghe, J., Renssen, H., Van Huissteden, J., Nugteren, G., Konert, M., Lu, H., Dodonov, A., Buylaert, J.-P., 2006. Penetration of Atlantic westerly winds into Central and East Asia. Quaternary Science Reviews 25, 2380–2389.
Vriend, M., Prins, M.A., Buylaert, J.P., Vandenberghe, J., Lu, H., 2011. Contrasting dust supply patterns across the north-western Chinese Loess Plateau during the last glacial-interglacial cycle. Quaternary International 240, 167–180.
Wang, F., Li, H.C., Zhu, R.X., Qin, F.Z., 2004. Late Quaternary down cutting rates of the Qianyou River from U/Th speleothem dates, Qinling Mountains, China. Quaternary Research 62, 194–200.
Wang, G.Z., 1984. A sketch of Quaternary glaciation in Eastern Qinling. Geology of Shaanxi 2, 47–65 (in Chinese).
Wang, S.J., 2005. Perspectives on Hominid Behaviour and Settlement Patterns: A Study of the Lower Palaeolithic Sites in the Luonan Basin, China. In: BAR International Series 1406. Archaeopress, Oxford, 1–248 pp.
Wang, S.J., Cosgrove, R., Lu, H.Y., Shen, C., Wei, M., Zhang, X.B., 2008a. New progress on Paleolithic archaeological studies in the Luonan Basin, China. In: Kazuto, Matsufuji (Ed.), Loess-paleosol and Paleolithic Chronology in East Asia. Yuzankaku, Tokyo, pp. 145–161 (in Japanese, with English Abstr.).
Wang, S.J., Lu, H.Y., Zhang, H.Y., Zhao, J., Cosgrove, R., Yi, S.W., Sun, X.F., Wei, M., Garvey, J., Ma, X.L., 2008b. A preliminary survey of Paleolithic artifacts and loess deposition in the middle South Luo River, Eastern Qinling Mountains, central China. Quaternary Sciences 28, 988–999 (in Chinese, with English Abstr.).
Weissmann, G.S., Hartley, A.J., Nichols, G.J., Scuderi, L.A., Olson, M., Buehler, H., Banteah, R., 2010. Fluvial form in modern continental sedimentary basins: distributive fluvial systems. Geology 38, 39–42.
Yang, J.D., Li, G.J., Rao, W.B., Ji, J.F., 2009. Isotopic evidences for provenance of East Asian dust. Atmospheric Environment 43, 4481–4490.
Yang, S.L., Fang, X.M., Shi, Z.T., Lehmkuhl, F., Song, C.H., Han, Y.X., Han, W.X., 2010. Timing and provenance of loess in the Sichuan Basin, southwestern China. Palaeogeography, Palaeoclimatology, Palaeoecology 292, 144–154.
Yang, S.Y., Li, C.X., Yang, D.Y., Li, X.S., 2004. Chemical weathering of the loess deposits in the lower Changjiang Valley, China, and paleoclimatic implications. Quaternary International 117, 27–34.
Yang, X.P., Liu, Y.S., Li, C.Z., Song, Y.L., Zhu, H.P., Jin, X.D., 2007a. Rare earth elements of aeolian deposits in Northern China and their implications for determining the provenance of dust storms in Beijing. Geomorphology 87, 365–377.
Yang, X.P., Zhu, B., White, P., 2007b. Provenance of aeolian sediment in the Taklamakan Desert of western China, inferred from REE and major-elemental data. Quaternary International 175, 71–85.
Yang, X.P., Zhang, F., Fu, X.D., Wang, X.M., 2008. Oxygen isotopic compositions of quartz in the sand seas and sandy lands of northern China and their implications for understanding the provenances of aeolian sands. Geomorphology 102, 278–285.
Yang, X.P., Scuderi, L., 2010. Hydrological and climatic changes in deserts of China since the Late Pleistocene. Quaternary Research 73, 1–9.
Yang, X.P., Scuderi, L., Paillou, P., Liu, Z.T., Li, H.W., Ren, X.Z., 2011. Quaternary environmental changes in the drylands of China – a critical review. Quaternary Science Reviews 30, 3219–3233.
Zhang, G.W., Meng, Q.R., Yu, Z.P., Sun, Y., Zhou, D.W., Guo, A.L., 1996. Orogenic processes and dynamics of the Qinling. Science in China (Series D) 39, 225–234.
Zhang, H.Y., Lu, H.Y., Zhao, J., Zhao, C.F., Zhang, P., 2008. The effects of ultrasonic dispersion on granulometry results of the fine-grain loess. Acta Sedimentologica Sinica 26, 494–500 (in Chinese, with English Abstr.).
Zhang, P., Liu, W.G., Lu, H.Y., Zhou, W.J., Zhao, C.F., 2009. Organic carbon isotope composition of Luonan loess compared with Luochuan and Xifeng loess. Quaternary Sciences 29, 34–41 (in Chinese, with English Abstr.).
Zhang, Z.H., Zhao, M.X., Lu, H.Y., Faiia, A.M., 2003. Lower temperature as the main cause of C_4 plant declines during the glacial periods on the Chinese Loess Plateau. Earth and Planetary Science Letters 214, 467–481.
Zhang, Z.Q., Zhang, G.W., Liu, D.Y., Wang, Z.Q., Tang, S.H., Wang, J.H., 2006. Isotopic Geochronology and Geochemistry of Ophiolites, Granites and Clastic Sedimentary Rocks in the Qinling Orogenic Belt. The Geological Publishing House, Beijing, 1–348 pp. (in Chinese).
Zhao, J., Lu, H.Y., Wang, X.Y., Zhang, H.Y., Wang, S.J., 2008. Magnetic properties of the loess deposit in Eastern Qinling Mountains and an investigation on the magnetic susceptibility enhancement. Acta Sedimentologica Sinica 26, 1052–1062 (in Chinese, with English Abstr.).
Zheng, H., Ji, J., Huang, X., Liu, R., Zeng, Q., Jiang, F., 2007. Ultra-high rates of loess sedimentation at Zhengzhou since Stage 7: implication for the yellow River running through the Sanmen Gorge. Geomorphology 85, 131–142.